Exact Analysis of Class E Tuned Power Amplifier at any Q and Switch Duty Cycle

MARIAN K. KAZIMIERCZUK AND KRZYSZTOF PUCZKO

Abstract—Previous analytical descriptions of a Class E high-efficiency switching-mode tuned power amplifier have been based on the assumption of an infinite Q or the minimum possible value of Q. This paper presents an exact analysis of the Class E amplifier at any Q and any switch duty cycle D, along with experimental results. The basic equations governing the amplifier operation are derived analytically using Laplace-transform techniques and assuming a constant current through the dc-fed choke. The following performance parameters are determined for optimum operation: the current and voltage waveforms, the peak collector current and collector–emitter voltage, the output power, the power-output capability, the load-network component values, and the spectrum of the output voltage. It is shown that all parameters of the amplifier are functions of Q. Therefore, the high-Q assumption used in previous analyses leads to considerable errors. For example, for $Q<7$ at $D=0.5$, some errors are up to 60 percent. The results can be used for designing Class E stages at any Q and switch duty cycle D. The measured performance shows excellent agreement with the design calculations. The collector efficiency was over 96 percent at 2 MHz for all tested values of Q from 0.1 to 10.

I. Introduction

Class E switching-mode tuned power amplifiers offer extremely high dc-to-ac conversion efficiency (e.g., 96 percent) because of a significant reduction in switching losses [1]–[23]. These amplifiers can be applied in practice, e.g., as power stages in communication equipment or in dc/dc power converters [24]–[27]. Class E frequency multipliers can also be realized [28], [29]. Previous analyses of the Class E amplifier have been performed analytically under the assumption of an infinite loaded quality factor Q [3], [15], [16] or the minimum possible value of Q [23], and an analysis given in [2] has been made numerically for any Q. The purpose of this paper is to present an analytical analysis of the Class E amplifiers at any Q and any switch ON duty cycle D, using Laplace-transform methods.

The basic circuit of the Class E amplifier and its equivalent circuit are shown in Fig. 1(a) and (b), respectively. The amplifier circuit consists of a single transistor (a BJT or a FET), a load network, and an RF choke (RFC). The transistor is driven to act periodically as a switch at the operating frequency f with switch ON duty cycle (D). The simplest type of the load network consists of the series circuit R, L, and C (resonant at a frequency lower than f) and the shunt capacitance C_1. The resistor R is a load to which the ac power is to be delivered. One of the important advantages of the amplifier topology is that all parasitic shunt capacitances, including the output transistor capacitance, are absorbed into C_1. The inductance of the RF choke is usually high enough so that the ac current is small compared to the dc current, but that is not a requirement on the design. Fig. 2 shows the current and voltage waveforms in the amplifier at high Q.

Manuscript received February 6, 1986.
M. K. Kazimierczuk is with the Department of Electrical Systems Engineering, Wright State University, Dayton, OH 45435, on leave from the Department of Electronics, Institute of Radio Electronics, Technical University of Warsaw, 00-665 Warsaw, Poland.
K. Puczko is with the Department of Electronics, Institute of Radio Electronics, Technical University of Warsaw, 00-665 Warsaw, Poland.
IEEE Log Number 8611458.

II. Analysis

A. Assumptions

The analysis given below is based on the equivalent circuit of the amplifier shown in Fig. 1(b) and the following assumptions.

1) The transistor acts as an ideal switch, i.e., it has zero saturation resistance, zero saturation voltage, infinite OFF resistance, and zero switching times.

2) The load network components C_1, C, and L are ideal, i.e., they are linear, lossless, and do not have parasitic resonances. The shunt capacitance C_1 includes the transistor output capacitance, the winding capacitance of the RF choke, and the stray wiring capacitance. The transistor output capacitance is independent of the collector-to-emitter voltage.

3) The RF choke is lossless and its inductance is high enough so that the current through it is constant and equal to the dc supply current I_{CC}.

B. Parameters

The following parameters of the equivalent circuit of Fig. 1(b) are defined below. When the switch is on, the series-resonant circuit consists of L, C, and R. Then the resonant frequency ($\omega_{01}=2\pi f_{01}$) and the loaded Q-factor (Q_1) are, respectively,

$$\omega_{01}=\frac{1}{\sqrt{LC}} \tag{1}$$

$$Q_1=\frac{\omega_{01}L}{R}=\frac{1}{\omega_{01}RC}. \tag{2}$$

0098-4094/87/0200-0149$01.00

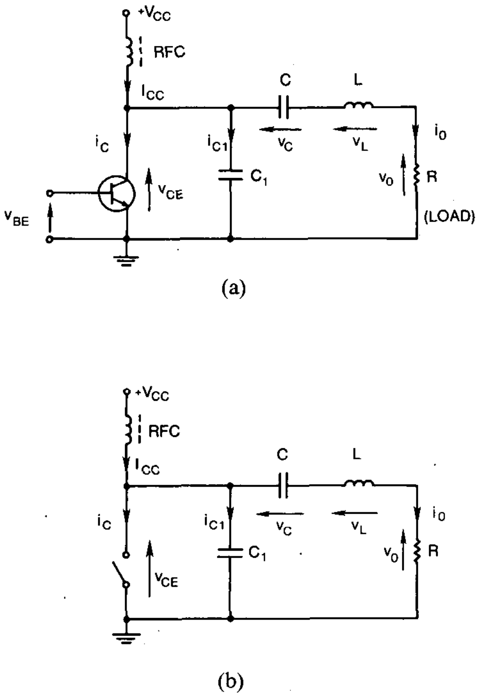

Fig. 1. Class E tuned power amplifier. (a) Basic circuit. (b) Equivalent circuit.

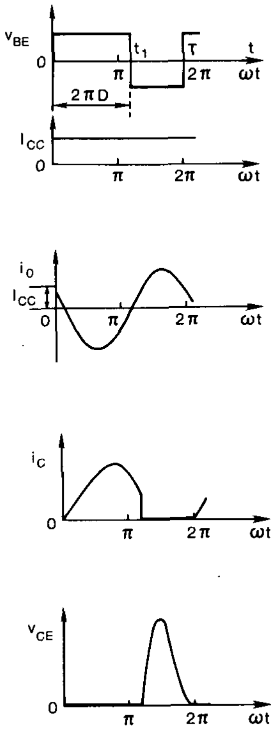

Fig. 2. Waveforms in the Class E amplifier for optimum operation at high Q.

When the switch is off, the series-resonant circuit consists of C_1, C, L, and R. Then the resonant frequency ($\omega_{02} = 2\pi f_{02}$) and the loaded Q-factor (Q_2) are, respectively,

$$\omega_{02} = \frac{1}{\sqrt{\frac{LCC_1}{C_1 + C}}} \tag{3}$$

$$Q_2 = \frac{\omega_{02} L}{R} = \omega_{02} R \frac{CC_1}{C + C_1}. \tag{4}$$

The operating (switching) frequency $f = \omega/(2\pi)$ differs from both resonant frequencies f_{01} and f_{02}. Therefore, it is convenient to introduce the following ratios of frequencies:

$$A_1 = \frac{f_{01}}{f} \tag{5}$$

$$A_2 = \frac{f_{02}}{f}. \tag{6}$$

From (1)–(6), we find

$$\frac{Q_1}{Q_2} = \frac{\omega_{01}}{\omega_{02}} = \frac{A_1}{A_2} = \sqrt{\frac{C_1}{C_1 + C}}. \tag{7}$$

The loaded Q-factor (Q_L) at the operating frequency f introduced in previous papers [3], [4] is

$$Q_L = \frac{\omega L}{R} = \frac{Q_1}{A_1} = \frac{Q_2}{A_2}. \tag{8}$$

The subsequent analysis will use the parameters Q_1, A_1, and A_2. The two remaining parameters, Q_2 and Q_L, can be calculated from (7) and (8).

C. Steady-State Waveforms

The basic equations for the equivalent circuit of the amplifier shown in Fig. 1 (b) are

$$i_C = I_{CC} - i_{C1} - i_o \tag{9}$$

$$v_{CE} = v_L + v_C + v_o. \tag{10}$$

In order to determine the waveforms in the circuit, two cases must be considered:

1) the *underdamped* case when $Q_1 > 0.5$,
2) the *overdamped* case when $Q_1 \leqslant 0.5$.

The steady-state waveforms of the collector current, collector-to-emitter voltage, and output voltage for $Q_1 > 0.5$

are derived in the Appendix. The results are as follows:

$$\frac{i_C}{I_{CC}}=\begin{cases}1-\exp\left(\frac{-A_1}{2Q_1}\omega t\right)\left[b_1\cos\left(\omega t A_1\sqrt{1-\frac{1}{4Q_1^2}}\right)-b_2\sin\left(\omega t A_1\sqrt{1-\frac{1}{4Q_1^2}}\right)\right] & \text{for } 0<\omega t\leqslant 2\pi D\\ 0 & \text{for } 2\pi D<\omega t\leqslant 2\pi\end{cases}\tag{11}$$

$$\frac{v_{CE}}{V_{CC}}=\begin{cases}0 & \text{for } 0<\omega t\leqslant 2\pi D\\ \frac{Q_1A_1}{a}\left[1-\left(\frac{A_1}{A_2}\right)^2\right]\left\{(\omega t-2\pi D)+\frac{1}{A_1^2}\left\{\exp\left(\frac{-A_1(\omega t-2\pi D)}{2Q_1}\right)\right.\right. & \\ \quad\left[h_3\cos\left[(\omega t-2\pi D)A_2\sqrt{1-\left(\frac{A_1}{2Q_1A_2}\right)^2}\right]\right. & \\ \quad\left.\left.\left.-h_4\sin\left[(\omega t-2\pi D)A_2\sqrt{1-\left(\frac{A_1}{2Q_1A_2}\right)^2}\right]\right]-h_3\right\}\right\} & \text{for } 2\pi D<\omega t\leqslant 2\pi\end{cases}\tag{12}$$

$$\frac{v_o}{V_{CC}}=\begin{cases}\frac{1}{a}\exp\left(\frac{-A_1\omega t}{2Q_1}\right)\left[b_1\cos\left(\omega t A_1\sqrt{1-\frac{1}{4Q_1^2}}\right)\right. & \\ \quad\left.-b_2\sin\left(\omega t A_1\sqrt{1-\frac{1}{4Q_1^2}}\right)\right] & \text{for } 0<\omega t\leqslant 2\pi D\\ \frac{1}{a}\left[1-\left(\frac{A_1}{A_2}\right)^2\right]+\frac{1}{a}\exp\left(-\frac{A_1(\omega t-2\pi D)}{2Q_1}\right) & \\ \quad\cdot\left\{h_1\cos\left[(\omega t-2\pi D)A_2\sqrt{1-\left(\frac{A_1}{2Q_1A_2}\right)^2}\right]\right. & \\ \quad\left.-h_2\sin\left[(\omega t-2\pi D)A_2\sqrt{1-\left(\frac{A_1}{2Q_1A_2}\right)^2}\right]\right\} & \text{for } 2\pi D<\omega t\leqslant 2\pi\end{cases}\tag{13}$$

where

$$b_1=1-\left(\frac{A_1}{A_2}\right)^2+(h_1\cos\theta_2-h_2\sin\theta_2)\cdot\exp\left[\frac{-\pi A_1(1-D)}{Q_1}\right]\tag{14}$$

$$b_2=\frac{b_1}{\tan\theta_1}-\frac{1-\left(\frac{A_1}{A_2}\right)^2+h_1}{\sin Q_1\exp\left(\frac{-\pi DA_1}{Q_1}\right)}\tag{15}$$

$$h_1=\frac{k_3m_1-k_1m_3}{k_3m_2+k_2m_3}\tag{16}$$

$$h_2=\frac{k_1+h_1k_2}{k_3}\tag{17}$$

$$h_3=h_1\frac{A_1}{2Q_1}-h_2A_2\sqrt{1-\left(\frac{A_1}{2Q_1A_2}\right)^2}\tag{18}$$

$$h_4=h_1A_2\sqrt{1-\left(\frac{A_1}{2Q_1A_2}\right)^2}+h_2\frac{A_1}{2Q_1}\tag{19}$$

$$h_5=\frac{h_1A_1A_2}{Q_1}\sqrt{1-\left(\frac{A_1}{2Q_1A_2}\right)^2}-h_2\left(A_2^2-\frac{A_1^2}{2Q_1^2}\right)\tag{20}$$

$$h_6=\frac{h_2A_1A_2}{Q_1}\sqrt{1-\left(\frac{A_1}{2Q_1A_2}\right)^2}+h_1\left(A_2^2-\frac{A_1^2}{2Q_1^2}\right)\tag{21}$$

$$m_1=\left[1-\left(\frac{A_1}{A_2}\right)^2\right]\left\{\frac{\sqrt{1-\frac{1}{4Q_1^2}}}{A_1\sin\theta_1}\cdot\left[\cos\theta_1-\frac{1}{\exp\left(\frac{-\pi DA_1}{Q_1}\right)}\right]+\frac{1}{2Q_1A_1}-2\pi(1-D)\right\}\tag{22}$$

$$m_2=\exp\left[\frac{-\pi A_1(1-D)}{Q_1}\right]\cdot\left\{\frac{\sqrt{1-\left(\frac{A_1}{2Q_1A_2}\right)^2}}{A_2}\sin\theta_2-\left(\frac{A_1}{2Q_1A_2^2}+\frac{\sqrt{1-\frac{1}{4Q_1^2}}}{A_1\tan\theta_1}-\frac{1}{2Q_1A_1}\right)\cos\theta_2\right\}+\frac{\sqrt{1-\frac{1}{4Q_1^2}}}{A_1\sin\theta_1\exp\left(\frac{-\pi DA_1}{Q_1}\right)}+\frac{A_1}{2Q_1A_2^2}-\frac{1}{2Q_1A_1} \tag{23}$$

$$m_3=\exp\left[\frac{-\pi A_1(1-D)}{Q_1}\right]\left\{\frac{\sqrt{1-\left(\frac{A_1}{2Q_1A_2}\right)^2}}{A_2}\cos\theta_2+\left(\frac{A_1}{2Q_1A_2^2}+\frac{\sqrt{1-\frac{1}{4Q_1^2}}}{A_1\tan\theta_1}-\frac{1}{2Q_1A_1}\right)\sin\theta_2\right\}+\left(\frac{A_2}{A_1^2}-\frac{1}{A_2}\right)\sqrt{1-\left(\frac{A_1}{2Q_1A_2}\right)^2} \tag{24}$$

$$k_1=\left[1-\left(\frac{A_1}{A_2}\right)^2\right]\left[\frac{\sqrt{1-\frac{1}{4Q_1^2}}\exp\left(\frac{-\pi DA_1}{Q_1}\right)}{A_1\sin\theta_1}-\frac{\sqrt{1-\frac{1}{4Q_1^2}}}{A_1\tan\theta_1}+\frac{1}{2Q_1A_1}\right] \tag{25}$$

$$k_2=\frac{\sqrt{1-\frac{1}{4Q_1^2}}}{A_1\sin\theta_1}\left[\cos\theta_2\exp\left(\frac{-\pi A_1}{Q_1}\right)-\cos\theta_1\right] \tag{26}$$

$$k_3=\frac{A_2\sqrt{1-\left(\frac{A_1}{2Q_1A_2}\right)^2}}{A_1^2}+\frac{\sqrt{1-\frac{1}{4Q_1^2}}\sin\theta_2\exp\left(\frac{-\pi A_1}{Q_1}\right)}{A_1\sin\theta_1} \tag{27}$$

$$a=Q_1\left(A_2^2-A_1^2\right)\left\{\frac{\pi A_1(1-D)^2}{A_2^2}+\frac{(1-D)\left(h_2A_2\sqrt{1-\frac{A_1^2}{4Q_1^2A_2^2}}-\frac{h_1A_1}{2Q_1}\right)}{A_2^2A_1}+\frac{\exp\left(\frac{-\pi A_1(1-D)}{Q_1}\right)(h_5\sin\theta_1+h_6\cos\theta_1)-h_6}{2\pi A_1A_2^4}\right\} \tag{28}$$

$$\theta_1=2\pi DA_1\sqrt{1-\frac{1}{4Q_1^2}} \tag{29}$$

$$\theta_2=2\pi A_2(1-D)\sqrt{1-\left(\frac{A_1}{2Q_1A_2}\right)^2}. \tag{30}$$

The "optimum turn-on conditions" are $v_{CE}=0$ and $dv_{CE}/d(\omega t)=0$ at $\omega t=2\pi$ [1]–[7]. Substitution of these conditions into (12) yields the relationship among Q_1, A_1, A_2, and D, which are given by the following system of equations:

$$2\pi(1-D)\left(\frac{A_1}{A_2}\right)^2-h_1\left[\exp\left(\frac{-\pi A_1(1-D)}{Q_1}\right)\cdot\left(\frac{\sin\theta_2\sqrt{1-\left(\frac{A_1}{2Q_1A_2}\right)^2}}{A_2}-\frac{A_1\cos\theta_2}{2Q_1A_2^2}\right)+\frac{A_1}{2Q_1A_2^2}\right]+h_2\left\{\frac{\sqrt{1-\left(\frac{A_1}{2Q_1A_2}\right)^2}}{A_2}-\exp\left[\frac{-\pi A_1(1-D)}{Q_1}\right]\cdot\left(\frac{A_1\sin\theta_2}{2Q_1A_2^2}+\frac{\cos\theta_2\sqrt{1-\left(\frac{A_1}{2Q_1A_2}\right)^2}}{A_2}\right)\right\}=0 \tag{31}$$

$$\left(\frac{A_1}{A_2}\right)^2-(h_1\cos\theta_2-h_2\sin\theta_2)\exp\left[\frac{-\pi A_1(1-D)}{Q_1}\right]=0. \tag{32}$$

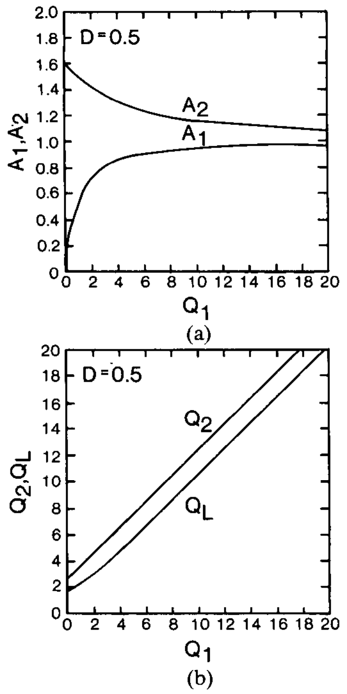

Fig. 3. Relationships among Q_1, Q_2, Q_L, A_1, and A_2 for $D = 0.5$. (a) A_1 and A_2 as functions of Q_1. (b) Q_2 and Q_L as functions of Q_1.

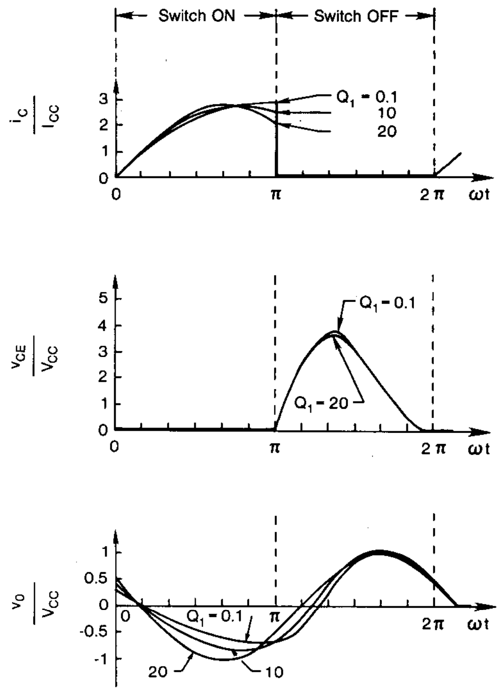

Fig. 4. Waveforms of i_C, v_{CE}, and v_o for optimum operation at $D = 0.5$ and $Q_1 = 0.1$, 10, and 20.

TABLE I
Q_1, Q_L, A_1, AND A_2 AS FUNCTIONS OF Q_1 AND D

Q_1	D = 0.25				D = 0.5				D = 0.75			
	Q_2	Q_L	A_1	A_2	Q_2	Q_L	A_1	A_2	Q_2	Q_L	A_1	A_2
0	4.965	4.445	0	1.117	2.866	1.788	0	1.603	2.612	0.821	0	3.182
1	5.141	4.619	0.2165	1.113	3.247	2.104	0.4752	1.543	3.715	1.247	0.8018	2.979
2	5.616	5.093	0.3927	1.103	4.124	2.850	0.7018	1.447	6.017	2.161	0.9256	2.785
3	6.292	5.765	0.5204	1.091	5.146	3.750	0.8001	1.372	8.302	3.157	0.9502	2.630
5	7.946	7.413	0.6745	1.072	7.242	5.673	0.8814	1.277	12.345	5.171	0.9670	2.387
7	9.777	9.239	0.7577	1.058	9.321	7.642	0.9160	1.220	15.877	7.182	0.9747	2.211
10	12.645	12.102	0.8263	1.045	12.405	10.621	0.9416	1.168	20.699	10.192	0.9812	2.021
15	17.576	16.994	0.8826	1.032	17.488	15.605	0.9612	1.121	27.590	15.201	0.9868	1.815
20	22.492	21.940	0.9116	1.025	22.536	20.597	0.9710	1.094	33.969	20.207	0.9898	1.681
100	102.37	101.81	0.9822	1.006	102.68	100.58	0.9942	1.021	119.78	100.22	0.9978	1.195
∞	∞	∞	1	1	∞	∞	1	1	∞	∞	1	1

For the overdamped case when $Q_1 \leqslant 0.5$, the terms $\sin\theta_1$, $\cos\theta_1$, $\tan\theta_1$, $\sqrt{1-1/4Q_1^2}$, $\sin(\omega t A_1\sqrt{1-1/4Q_1^2})$, and $\cos(\omega t A_1\sqrt{1-1/4Q_1^2})$ must be replaced in (11)–(32) by $\sinh\theta_1$, $\cosh\theta_1$, $\tanh\theta_1$, $\sqrt{1/4Q_1^2-1}$, $\sinh(\omega t A_1\sqrt{1/4Q_1^2-1})$, and $\cosh(\omega t A_1\sqrt{1/4Q_1^2-1})$, respectively.

The system of equations (31) and (32) was solved numerically by Newton's method and then Q_2 was computed from (7). The results are shown in Fig. 3 for $D = 0.5$ and in Table I for $D = 0.25$, 0.5, and 0.75. The theoretical range of Q_1 is from zero to infinity. For $Q_1 = 0$ at $D = 0.5$, $A_1 = 0$, $A_2 = 1.603$, $Q_2 = 2.866$, and $Q_L = 1.7879$; then C becomes an ideal blocking capacitor [23]. As $Q_1 \to \infty$, both A_1 and $A_2 \to 1$ (i.e., $f \to f_{01} \to f_{02}$) and both Q_2 and $Q_L \to \infty$.

The practical range of Q_1, typically, is from 1 to 20. The lowest value of Q_1 is limited by the size of C. The highest value of Q_1 is limited by the efficiency of the load network $\eta_{LN} = 1 - Q_L/Q_o$, where Q_o is the quality factor of L at the operating frequency f.

Substituting Q_1, A_1, and A_2, given in Table I, into (11)–(13), we obtain the waveforms of i_C, v_{CE}, and v_o for optimum operation. Fig. 4 shows the waveforms for $Q_1 = 0.1$, 10, and 20 at $D = 0.5$.

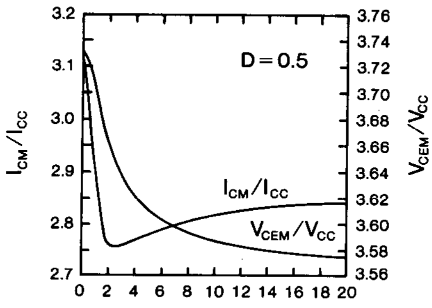

Fig. 5. Normalized peak collector current and peak collector–emitter voltage as functions of Q_1 for $D = 0.5$.

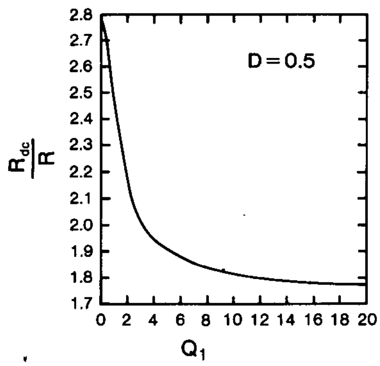

Fig. 6. Resistance ratio R_{dc}/R as a function of Q_1 for $D = 0.5$.

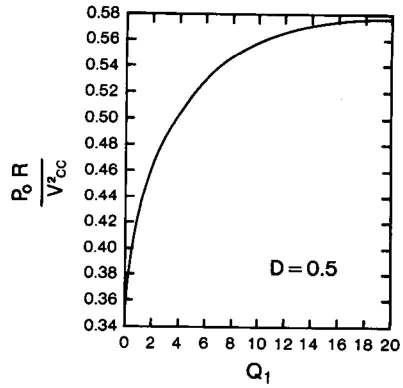

Fig. 7. Normalized output power as a function of Q_1 for $D = 0.5$.

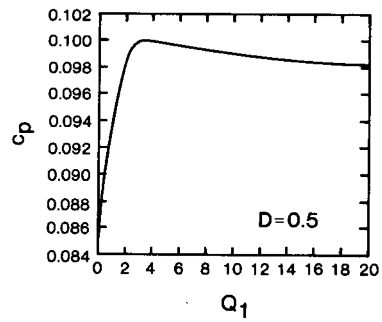

Fig. 8. Power-output capability as a function of Q_1 for $D = 0.5$.

TABLE II
AMPLIFIER PARAMETERS AS FUNCTIONS OF Q_1 AND D

Q_1	D = 0.25				D = 0.5				D = 0.75			
	$\frac{I_{CM}}{I_{CC}}$	$\frac{V_{CEM}}{V_{CC}}$	$\frac{P_oR}{V_{CC}^2}$	c_p	$\frac{I_{CM}}{I_{CC}}$	$\frac{V_{CEM}}{V_{CC}}$	$\frac{P_oR}{V_{CC}^2}$	c_p	$\frac{I_{CM}}{I_{CC}}$	$\frac{V_{CEM}}{V_{CC}}$	$\frac{P_oR}{V_{CC}^2}$	c_p
0	7.556	2.472	0.0410	0.0535	3.128	3.732	0.3587	0.0857	1.608	7.485	1.630	0.0831
1	7.515	2.469	0.0417	0.0539	2.886	3.703	0.4008	0.0936	1.730	7.357	1.637	0.0786
2	7.392	2.463	0.0432	0.0549	2.761	3.662	0.4570	0.0989	1.909	7.262	1.798	0.0721
3	7.295	2.456	0.0450	0.0558	2.759	3.636	0.4916	0.0997	1.981	7.219	1.729	0.0699
5	7.166	2.445	0.0481	0.0571	2.783	3.610	0.5249	0.0996	2.040	7.177	1.658	0.0683
7	7.044	2.437	0.0503	0.0583	2.800	3.597	0.5401	0.0993	2.068	7.158	1.621	0.0676
10	6.974	2.430	0.0524	0.0590	2.816	3.587	0.5514	0.0990	2.090	7.143	1.592	0.0670
20	6.850	2.419	0.0555	0.0603	2.837	3.574	0.5644	0.0986	2.119	7.126	1.553	0.0662
100	6.741	2.409	0.0586	0.0616	2.857	3.565	0.5744	0.0982	2.144	7.114	1.518	0.0655
∞	6.799	2.407	0.0595	0.0611	2.862	3.565	0.5768	0.0981	2.151	7.112	1.508	0.0654

The peak collector current I_{CM} and peak collector–emitter voltage V_{CEM} were computed numerically from (11) and (12). The results are shown in Fig. 5 for $D = 0.5$ and in Table II for $D = 0.25$, 0.5, and 0.75. It is seen that I_{CM} and V_{CEM} are almost independent of Q_1.

D. Energy Parameters

The dc resistance which the amplifier presents to the dc power supply is

$$R_{dc} = \frac{V_{CC}}{I_{CC}} = aR \tag{33}$$

where a is given by (28). Ratio R_{dc}/R is illustrated in Fig. 6. For $D = 0.5$, it decreases from 2.780 at $Q_1 = 0$ to 1.734 as $Q_1 \to \infty$. The variation of R_{dc}/R normalized to 1.734 is 60.3 percent.

The dc power input is $P_{CC} = I_{CC}V_{CC}$. The collector efficiency under the assumptions 1)–3) is 100 percent. Therefore, the output power $P_o = P_{CC}$. Hence,

$$P_o = \frac{V_{CC}^2}{R_{dc}} = \frac{V_{CC}^2}{aR}. \tag{34}$$

The normalized output power $P_oR/V_{CC}^2 = 1/a = R/R_{dc}$ is

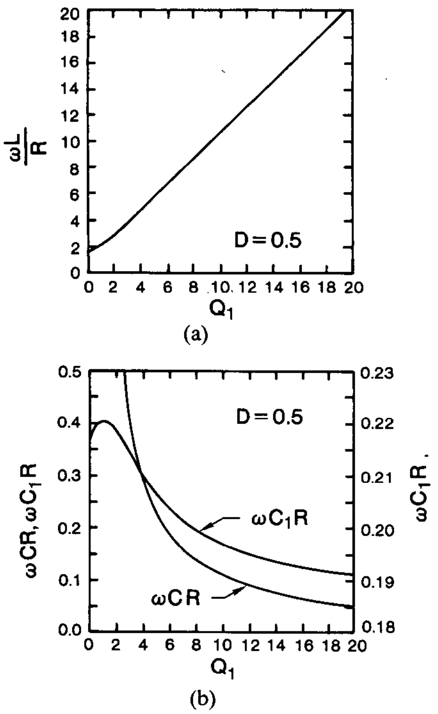

Fig. 9. Relationships among the load-network components for $D = 0.5$. (a) $\omega L/R$ as a function of Q_1. (b) ωCR and $\omega C_1 R$ as functions of Q_1.

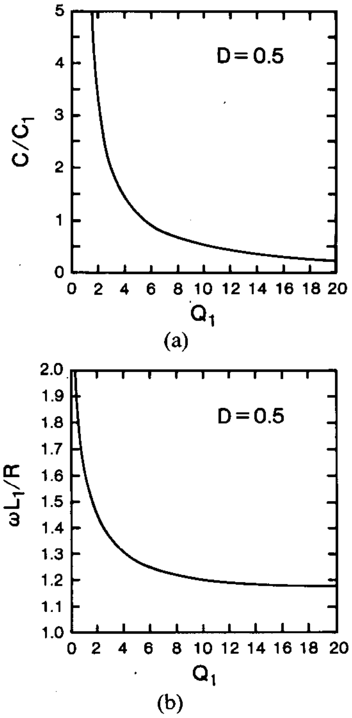

Fig. 10. (a) C/C_1 as a function of Q_1 at $D = 0.5$. (b) $\omega L/R$ as a function of Q_1 at $D = 0.5$.

TABLE III
LOAD-NETWORK COMPONENT VALUES AS FUNCTIONS OF Q_1 AND D

Q_1	D = 0.25: $\frac{\omega L}{R}$	D = 0.25: ωRC	D = 0.25: ωRC_1	D = 0.5: $\frac{\omega L}{R}$	D = 0.5: ωRC	D = 0.5: ωRC_1	D = 0.75: $\frac{\omega L}{R}$	D = 0.75: ωRC	D = 0.75: ωRC_1
0	4.445	∞	0.1803	1.788	∞	0.2177	0.8207	∞	0.1203
1	4.619	4.619	0.1817	2.104	2.104	0.2204	1.247	1.247	0.09741
2	5.093	1.273	0.1849	2.850	0.7124	0.2190	2.161	0.5402	0.06710
3	5.765	0.6405	0.1885	3.750	0.4166	0.2150	3.157	0.3508	0.05269
5	7.413	0.2965	0.1944	5.673	0.2269	0.2067	5.171	0.2068	0.04059
7	9.239	0.1815	0.1983	7.642	0.1560	0.2017	7.182	0.1466	0.03536
10	12.10	0.1210	0.2020	10.62	0.1062	0.1971	10.19	0.1019	0.03143
15	16.99	0.07553	0.2054	15.61	0.06936	0.1931	16.20	0.06329	0.02796
20	21.94	0.05485	0.2072	20.60	0.05149	0.1909	20.21	0.05052	0.02680
100	101.81	0.01018	0.2119	100.58	0.01006	0.1851	100.22	0.01002	0.02306
∞	∞	0	0.2132	∞	0	0.1836	∞	0	0.02211

shown in Fig. 7 and in Table II. $P_o R/V_{CC}^2$ increases from 0.3587 at $Q_1 = 0$ to $8/(\pi^2+4) = 0.5768$ as $Q_1 \to \infty$. The variation of its value normalized to 0.5768 is 37.8 percent.

The power-output capability is

$$c_p = \frac{P_o}{I_{CM} V_{CEM}} = \frac{I_{CC} V_{CC}}{I_{CM} V_{CEM}}. \tag{35}$$

Substituting I_{CM}/I_{CC} and V_{CEM}/V_{CC} into (35), we can calculate c_p. The results are shown in Fig. 8 and in Table II. For $D = 0.5$, c_p first increases rapidly with Q_1 starting from 0.0857 at $Q_1 = 0$, reaches its maximum value $c_{p\max} =$ 0.0997 at $Q_1 = 3$, then slowly decreases to 0.0981 as $Q_1 \to \infty$.

E. Relationships Among Load-Network Components

From (1)–(8), we obtain

$$\frac{\omega L}{R} = \frac{Q_1}{A_1} = Q_L \tag{36}$$

$$\omega CR = \frac{1}{Q_1 A_1} = \frac{1}{Q_L A_1^2} \tag{37}$$

$$\omega C_1 R = \frac{A_1}{Q_1 (A_2^2 - A_1^2)} = \frac{1}{Q_L (A_2^2 - A_1^2)}. \tag{38}$$

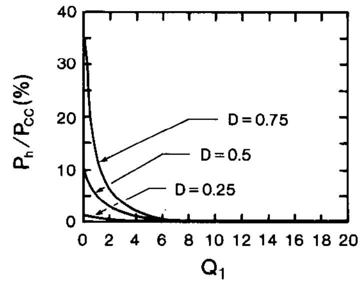

Fig. 11. Normalized output power of higher harmonics as a function of Q_1.

TABLE IV
HARMONIC COMPONENTS OF OUTPUT VOLTAGE AT $D = 0.5$

n	Q_1 = 0.05			Q_1 = 5			Q_1 = 20		
	$V_{o(n)}/V_{CC}$	$V_{o(n)}/V_{o(1)}$	$P_{o(n)}/P_{CC}$	$V_{o(n)}/V_{CC}$	$V_{o(n)}/V_{o(1)}$	$P_{o(n)}/P_{CC}$	$V_{o(n)}/V_{CC}$	$V_{o(n)}/V_{o(1)}$	$P_{o(n)}/P_{CC}$
1	0.8108	1.000	0.9134	1.020	1.000	0.9913	1.062	1.000	0.9993
2	0.2439	0.3008	0.08265	0.09405	0.09219	0.008425	0.02706	0.02548	0.0006486
3	0.04974	0.06134	0.003437	0.01486	0.01456	0.0002103	0.004047	0.003811	0.00001451
4	0.01672	0.02063	0.0003887	0.006073	0.005953	0.00003513	0.001797	0.001692	0.00000286
5	0.008377	0.01033	0.00009751	0.002771	0.002716	0.00000731	0.0007935	0.0007471	0.00000056
6	0.004543	0.005603	0.00002867	0.001717	0.001585	0.00000249	0.0004767	0.0004489	0.00000020
7	0.002863	0.003531	0.00001139	0.0009728	0.0009536	0.00000090	0.0002820	0.0002655	0.00000007
8	0.001862	0.002297	0.00000482	0.0006576	0.0006446	0.00000041	0.0001935	0.0001822	0.00000003
9	0.001312	0.001619	0.00000239	0.0004509	0.0004420	0.00000019	0.0001313	0.0001237	0.00000002
10	0.0009410	0.001161	0.00000123	0.0003311	0.0003245	0.00000010	0.0009733	0.0009164	0.00000001

These relationships are graphed in Fig. 9 and are tabulated in Table III. As Q_1 increases from zero to infinity at $D = 0.5$, $\omega L/R$ increases from 1.7879 to infinity, ωCR decreases from infinity to zero, and $\omega C_1 R$ decreases from 0.2177 to $8/[\pi(\pi^2+4)] = 0.1836$. The variation of $\omega C_1 R$ normalized to 0.1836 is 18.57 percent.

From (7), (37), and (38), $C/C_1 = (Q_2/Q_1)^2 - 1 = (A_2/A_1)^2 - 1$. Fig. 10(a) shows C/C_1 as a function of Q_1 at $D = 0.5$. As Q_1 increases from zero to infinity, C/C_1 decreases from infinity to zero.

In previous analyses [3], [15], [16], L is divided into two series inductances, L_r and L_1. L_r is resonant with C at the operating frequency f and $L_1 = L - L_r$. Hence, from (1), (7), and (8), $\omega L_1/R = Q_1/A_1 - Q_1 A_1 = Q_L(1 - A_1^2)$. Fig. 10(b) illustrates $\omega L_1/R$ as a function of Q_1 at $D = 0.5$. As Q_1 increases from zero to infinity, $\omega L_1/R$ decreases from infinity to $\pi(\pi^2 - 4)/16 = 1.1525$.

F. Spectrum of Output Voltage

Table IV shows the harmonic spectrum of v_o for $Q_1 =$ 0.05, 10, and 20 at $D = 0.5$. $V_{o(n)}/V_{CC}$ is the amplitude of the nth harmonic of v_o normalized to the dc supply voltage V_{CC}. $V_{o(n)}/V_{o(1)}$ is the amplitude of the nth harmonic of v_o normalized to the amplitude of the fundamental component of v_o. $P_{o(n)}/P_{CC}$ is the output power of the nth harmonic normalized to the dc input power. $V_{o(n)}/V_{o(1)}$ decreases with Q_1 and n, and increases with D.

From (33) and (34), the output power at the fundamental frequency f normalized to P_{CC} is $P_{o(1)}/P_{CC} = (V_{o(1)}V_{CC})^2 R_{dc}/(2R) = a(V_{o(1)}/V_{CC})^2/2$. Hence, the total output power at the higher harmonics (i.e., for $n \geq 2$) normalized to P_{CC} is $P_h/P_{CC} = 1 - P_{o(1)}/P_{CC}$. Fig. 11 shows P_h/P_{CC} as a function of Q_1 at $D = 0.25$, 0.5, and 0.75. For $Q_1 = 0$ at $D = 0.25$, 0.5, and 0.75, $P_h/P_{CC} = 0.99$, 8.66, and 34 percent, respectively. For $Q_1 = 5$ at $D = 0.25$, 0.5, and 0.75, $P_h/P_{CC} = 0.35$, 0.9, and 1.63 percent, respectively. It is seen that P_h/P_{CC} increases with D. However, for $Q_1 \geq 5$, P_h/P_{CC} is negligible.

III. EXPERIMENTAL RESULTS

The theoretical results were verified experimentally in the amplifier circuit of Fig. 1(a), using a BSX60 T0-39 transistor, $f = 2$ MHz, $D = 0.5$, $V_{CC} = 10$ V, $R = 50$ Ω, and $Q_1 = 10$, 5, 1, and 0.1. Fig. 12 shows the waveforms of i_C and v_{CE}. It is seen that the "optimum turn-on conditions" are satisfied for all values of Q_1. Fig. 13 shows the waveforms of v_o and i_C. According to the theoretical predictions, the output voltage is sinusoidal at high Q_1 and is nonsinusoidal at low Q_1. The collector efficiency measured with a thermistor probe was 96 percent. The measured values of the load-network components were in very good agreement with the theoretical predictions for all tested values of Q_1.

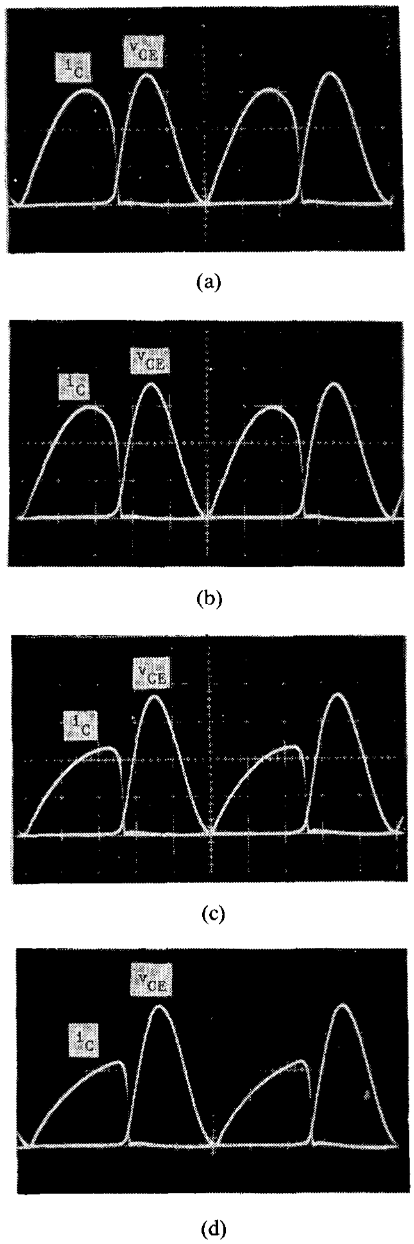

Fig. 12. Waveforms of the collector current and the collector–emitter voltage for $D=0.5$. (a) $Q_1=10$. (b) $Q_1=5$. (c) $Q_1=1$. (d) $Q_1=0.1$. Vertical: 0.1 A and 10 V/div.; horizontal: 100 ns/div.

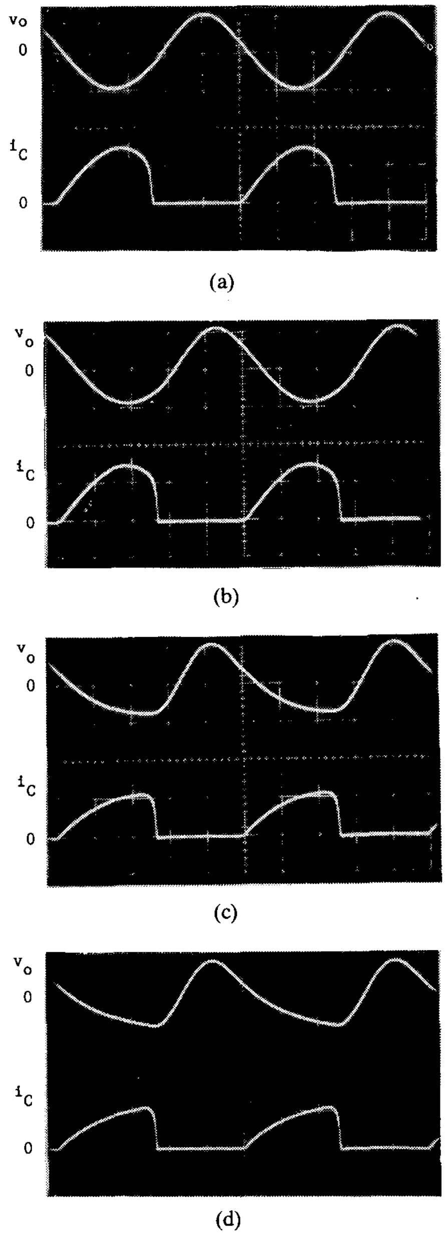

Fig. 13. Waveforms of the output voltage v_o and the collector current i_C for $D=0.5$. (a) $Q_1=10$. (b) $Q_1=5$. (c) $Q_1=1$. (d) $Q_2=0.1$. Vertical: 10 V and 0.2 A/div.; horizontal: 100 ns/div.

IV. Conclusions

An exact analysis of the Class E amplifier at any Q and switch duty cycle D has been presented. The design equations for optimum circuit operation have been derived, illustrated graphically, tabulated, and verified experimentally.

The following conclusions can be formulated.

1) The parameters of the Class E amplifier are functions of Q_1 and D.

2) The conditions for optimum circuit operation can be satisfied at any values of Q_1 and D.

3) The high-Q assumption leads to considerable errors if Q_1 is low. For example, for $D=0.5$, the values of $\omega C_1 R$, $P_o R/V_{CC}^2$, and R_{dc}/R at $Q_1=0$ and as $Q_1 \to \infty$ differ by 18.57, 37.8, and 60.3 percent, respectively.

4) The percentage differences decrease as Q_1 increases. For $D=0.5$, the values of $\omega C_1 R$, $P_o R/V_{CC}^2$, and R_{dc}/R at $Q=7$ and as $Q_1 \to \infty$ differ by 9.86, 6.66, and 6.8 percent, respectively, and at $Q_1=10$ and as $Q_1 \to \infty$, the differences are 1.12, 4.4, and 4.61 percent, respectively.

5) The effect of Q_1 should be taken into account in the design process for $Q_1 < 7$ at $D=0.5$. However, this effect can be neglected for $7 \leqslant Q_1 \leqslant 10$, as errors are found to be less than 10 percent, and for $Q_1 \geqslant 10$, the errors are less than 5 percent.

6) The switch ON duty cycle D should be greater than 0.25 because I_{CM}/I_{CC} is too high at low D ($I_{CM}/I_{CC} = 7.505$ at $D=0.25$ and $Q_1=0$), and D should be less than 0.75 because V_{CEM}/V_{CC} is too high at high D ($V_{CEM}/V_{CC} = 7.485$ at $D=0.75$ and $Q_1=0$). A more reasonable, practical range of Q_1 is from 0.4 to 0.6. For $D=0.4$ and

$Q_1 = 0$, $I_{CM}/I_{CC} = 4.270$ and $V_{CEM}/V_{CC} = 3.101$. For $D = 0.6$ and $Q_1 = 0$, $I_{CM}/I_{CC} = 2.357$ and $V_{CEM}/V_{CC} = 4.674$. The values of I_{CM}/I_{CC} and V_{CEM}/V_{CC} for $Q_1 = 0$ at any D are given in [23].

7) For $Q_1 \geqslant 5$ at $D = 0.5$, the output power approximately equals the output power at the fundamental frequency as the total output power at higher harmonics P_h/P_{CC} is less than 1 percent. Therefore, in Class E dc/dc power converters, only the power of the fundamental component is converted into the dc output power for $Q_1 \geqslant 5$ at $D = 0.5$ [27].

8) The amplitude of the nth harmonic of v_o normalized to the amplitude of the fundamental component $V_{o(n)}/V_{o(1)}$ increases with D and decreases with Q_1 and n. However, an output low-pass or bandpass filter should be added in applications of the Class E amplifier as an output-power stage in radio transmitters, as suggested in [5].

Appendix

Derivations of Current and Voltage Waveforms

When the switch is ON ($0 < t \leqslant t_1$), $v_{CE} = 0$ and $i_{C1} = 0$. Hence,

$$v_C + v_L + v_o = 0 \tag{A1}$$

$$i_C = I_{CC} - i_o. \tag{A2}$$

Using the Laplace-transform method, we find

$$I_o(s) = \frac{s i_o(0) - v_C(0)/L}{s^2 + 2\alpha s + \omega_{01}^2} \tag{A3}$$

where $i_o(0)$ and $v_C(0)$ are the initial conditions at $t = 0$, $\alpha = R/2L = \omega A_1/(2Q_1)$, and ω_{01} is given by (1).

When the switch is OFF ($t_1 < t \leqslant T$), $i_C = 0$. Therefore,

$$v_{CE} = v_C + v_L + v_o \tag{A4}$$

$$i_{C1} = I_{CC} - i_o. \tag{A5}$$

Hence,

$$V_{CE}(s) = I_o(s)\left(R + sL + \frac{1}{sC}\right) + \left[\frac{v_C(t_1)}{s} - L i_o(t_1)\right] e^{-st_1} \tag{A6}$$

$$I_o(s) = \frac{\left[I_{CC} + s^2 L C_1 i_o(t_1) - s C_1 v_C(t_1)\right] e^{-st_1}}{s L C_1 \left(s^2 + 2\alpha s + \omega_{02}^2\right)} \tag{A7}$$

where $i_o(t_1)$ and $v_C(t_1)$ are the initial conditions at $t = t_1$, and ω_{02} is given by (3). Solving (A3), (A6), and (A7), and taking into account that i_o and v_C are continuous and periodic functions, we can eliminate the initial conditions and determine the waveforms of i_C, v_{CE}, and v_o given by (11) to (13), respectively.

Acknowledgment

The authors wish to express their great appreciation to Prof. J. Ebert with the Department of Electronics, Technical University of Warsaw, Warsaw, Poland, for his professional and personal support of this project.

References

[1] N. O. Sokal and A. D. Sokal, "Class E—A new class of high-efficiency tuned single-ended switching power amplifiers," *IEEE J. Solid-State Circuits*, vol. SC-10, no. 3, pp. 168–176, June 1975. Reprinted in Japanese translation in *Nikkei Electronics*, pp. 127–141, Mar. 22, 1976.

[2] ____, "Class E switching-mode RF power amplifiers—Low power dissipation, low sensitivity to component tolerances (including transistors), and well-defined operation," presented at the IEEE ELECTRO/79 Conf., Session 23, New York, NY, Apr. 25 1979. Reprinted in *R. F. Design*, vol. 3., no. 7, pp. 33–38, 41, July/Aug. 1980.

[3] F. H. Raab, "Idealized operation of the Class E tuned power amplifier," *IEEE Trans. Circuits Syst.*, vol. CAS-24, pp. 725–735, Dec. 1977.

[4] ____, "Effects of circuit variations in the Class E tuned power amplifier," *IEEE J. Solid-State Circuits*, vol. SC-13, pp. 239–247, Apr. 1978.

[5] N. O. Sokal and F. H. Raab, "Harmonic output of Class E RF power amplifiers and load coupling network design," *IEEE J. Solid-State Circuits*, vol. SC-13, pp. 239–247, Apr. 1978.

[6] F. H. Raab and N. O. Sokal, "Transistor power losses in the Class E tuned power amplifiers," *IEEE J. Solid-State Circuits*, vol. SC-13, pp. 912–914, Dec. 1978.

[7] H. L. Krauss, C. W. Bostian, and F. H. Raab, *Solid State Radio Engineering*. New York: Wiley, 1980.

[8] V. V. Gruzdiev, "Calculation of circuit parameters of single-ended switching-mode tuned power amplifier" (in Russian), *Trudy MEIS*, vol. 2, pp. 124–128, 1969.

[9] G. Kuraishi, "Analysis of Class E RF power amplifier circuits" (in Japanese), *Trans. IECE Japan*, vol. J.60-B, no. 8, pp. 597–598, Aug. 1977.

[10] G. Kuraishi and F. Tajima, "Behavior analysis and circuit design of high efficiency power amplifiers in VHF band" (in Japanese), *Trans. IECE Japan*, vol. J.63-B, no. 10, pp. 999–1006, Oct. 1980.

[11] M. Kessous and J.-F. Zürcher, "A VHF Class E amplifier using a VMOS power FET" (in French), *Mitteilungen Commun.* (Switzerland), no. 30, pp. 45–49, Oct. 1980.

[12] J. Ebert and M. Kazimierczuk, "High efficiency RF power transistor amplifier," *Bull. Acad. Pol. Sci., Ser. Sci. Tech.*, vol. 25, no. 2, pp. 135–138, 1977.

[13] ____, "Class E high-efficiency tuned power oscillator," *IEEE J. Solid-State Circuits*, vol. SC-16, pp. 62–66, Apr. 1981.

[14] M. Kazimierczuk, "High-efficiency tuned transistor power amplifier" (in Polish), Ph.D. dissertation, Tech. Univ. Warsaw, Poland, 1977.

[15] ____, "Theory of the Class E tuned power amplifier" (in Polish), *Rozpr. Elektrot.*, vol. 25, no. 4, pp. 957–986, 1979.

[16] ____, "Theoretical analysis of the Class E tuned power amplifier at any switch duty ratio" (in Polish), *Rozpr. Elektrot.*, vol. 25, no. 4, pp. 987–1003, 1979.

[17] ____, "Effects of the collector current fall time on the Class E tuned power amplifier," *IEEE J. Solid-State Circuits*, vol. SC-18, pp. 181–193, Apr. 1983.

[18] ____, "Parallel operation of power transistors in switching amplifiers," *Proc. IEEE*, vol. 71, pp. 1456–1457, Dec. 1983.

[19] ____, "Collector amplitude modulation of the Class E tuned power amplifier," *IEEE Trans. Circuits Syst.*, vol. CAS-31, pp. 543–549, June 1984.

[20] ____, "High-efficiency tuned power amplifiers, frequency multipliers, and oscillators" (in Polish), Dr. Hab. dissertation, Tech. Univ. Warsaw, Poland, 1984.

[21] B. Molnár, "Basic limitations of waveforms achievable in single-ended switching-mode (Class E) power amplifiers," *IEEE J. Solid-State Circuits*, vol. SC-19, pp. 144–146, Feb. 1984.

[22] M. K. Kazimierczuk, "Generalization of conditions for 100-percent efficiency and nonzero output power in power amplifiers and frequency multipliers," *IEEE Trans. Circuits Syst.*, vol. CAS-33, pp. 805–807, Aug. 1986.

[23] ____, "Class E tuned power amplifier with nonsinusoidal output voltage," *IEEE J. Solid-State Circuits*, vol. SC-21, pp. 575–581, Aug. 1986.

[24] R. Redl, B. Molnár, and N. O. Sokal, "Class E resonant regulated dc/dc power converters: Analysis of operation and experimental results at 1.5 MHz," in *IEEE Power Electronics Specialists Conf. Rec.*, IEEE Publication 83CH1877-0, (Albuquerque, NM), June 6, 1983, pp. 50–60.

[25] R. Redl and B. Molnár, "Design of a 1.5-MHz regulated dc/dc power converter," in *Proc. 7th Int. PCI Conf. on Power Conversion* (Geneva, Switzerland), Sept. 1983, pp. 74–87.

[26] R. Redl, B. Molnár, and N. O. Sokal, "Small-signal dynamic analysis of regulated Class-E dc/dc converters," in *IEEE Power Electronics Specialists Conf. Rec.*, IEEE Publication 84CH2000-8, (Gaithersburg, MD), June 18, 1984, pp. 62–71.

[27] M. K. Kazimierczuk and K. Puczko, "Impedance inverter for Class E dc/dc resonant converter," in *Proc. 29th Midwest Symp. on Circuits and Systems* (Lincoln, NE), Aug. 11–12, 1986.

[28] V. B. Kozyrev, "Switching-mode transistor frequency multipliers" (in Russian), *Radiotekhnika*, vol. 30, no. 2, pp. 54–65, 1975.
[29] R. E. Zulinski and J. W. Steadman, "Performance evaluation of Class E frequency multipliers," *IEEE Trans. Circuits Syst.*, vol. CAS-33, pp. 343–346, Mar. 1986.

Marian K. Kazimierczuk was born in Poland on March 3, 1948. He received the M.S., Ph.D., and Habilitate Doctorate degrees in electronics engineering from the Department of Electronics, Technical University of Warsaw, Warsaw, Poland, in 1971, 1978, and 1984, respectively.

In 1972, he joined the Institute of Radio Electronics, Department of Electronics, Technical University of Warsaw, Warsaw, Poland, where he was employed as an Instructor from 1972 to 1978 and as an Assistant Professor from 1978 to 1984. He headed the Radio Electronics Laboratory and the Electronic Apparatus Laboratory from 1978 to 1984. His teaching, research, and development activities were in the areas of RF power technology, radio transmitters, electronic circuits and systems, semiconductor device modeling, electromagnetic field theory, microwave theory and techniques, electronic measurements, circuit theory, communications, and computer-aided design. In 1984, he worked as a Project Engineer at Design Automation, Inc., Lexington, MA, where he was responsible for designing Class E high-efficiency switching-mode DC/DC converters. In 1984/85, he was a Visiting Professor with the Department of Electrical Engineering, Virginia Polytechnic Institute and State University, Blacksburg, VA, where he taught electromagnetic fields and electronic circuits and systems, and his research activity was in the area of power electronics. Since 1985, he has been a Visiting Professor with the Department of Electrical Systems Engineering, Wright State University, Dayton, OH, where he has been working in the areas of analog and digital electronics, integrated circuits, electronic devices, and power electronics. He is the author of 45 scientific papers, of which 13 were published in IEEE Transactions and Journals. He also holds six patents related to the new concepts of high-efficiency switching-mode tuned power amplifiers and oscillators.

Dr. Kazimierczuk is a member of the Association of Polish Engineers and the Polish Society of Theoretical and Applied Electrical Sciences. He received seven awards from the president of the Technical University of Warsaw, three awards from the Polish Ministry of Science, University Education, and Technology in 1981, 1982, and 1985, and an award from the Polish Academy of Sciences in 1983 for scientific achievements.

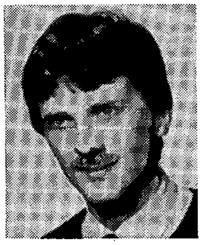

Krzysztof Puczko was born in Poland on April 8, 1961. He received the M.S. degree in electronics engineering from the Department of Electronics, Technical University of Warsaw, Warsaw, Poland, in 1986.

His research interests are in the areas of tuned power transistor amplifiers, resonant DC/DC power converters, and computer-aided design.